Electrical Properties of a Lead-Free Perovskite Ceramic: Ba(Gd$_{1/2}$Nb$_{1/2}$)O$_3$

K. Amar Nath[1], K.P. Chandra[2], A.R. Kulkarni[3], K. Prasad[*1]

[1]University Department of Physics, T.M. Bhagalpur University, Bhagalpur – 812 007, India

[2]Department of Physics, S.M. College, Bhagalpur – 812 001, India

[3]Department of Metallurgical Engineering and Materials Science, Indian Institute of Technology, Mumbai – 400 076, India

[1]karn190@gmail.com; [2]kpchandra23@gmail.com; [3]ajit.kulkarni@iitb.ac.in; [*1]k.prasad65@gmail.com

Abstract

Polycrystalline Ba(Gd$_{1/2}$Nb$_{1/2}$)O$_3$ was prepared using a high-temperature solid-state reaction method. X-ray diffraction analysis indicated the formation of a single-phase cubic structure having space group $Pm\overline{3}m$. AC impedance plots as a function of frequency at different temperatures were used to analyse the electrical behaviour of the sample, which indicated the negative temperature coefficient of resistance character. Complex impedance analysis targeted non-Debye type dielectric relaxation. Frequency dependent ac conductivity data obeyed Jonscher's power law. The apparent activation energy was estimated to be 0.17 eV at 1 kHz.

Keywords

Ba(Gd$_{1/2}$Nb$_{1/2}$)O$_3$; Perovskite; Dielectric Properties; Dielectric Relaxation; Electrical Conductivity

Introduction

In recent years, a number of perovskite ABO$_3$-type non/low-lead materials have been studied for various technological applications such as in multilayer capacitors, ferroelectric, piezoelectric, pyroelectric, memories, solid oxide fuel cells, energy harvesting, microwave, *etc*. In case of a cubic structure, the oxygen atoms form a cubic lattice of corner-sharing octahedra with B-cations at their centres while A-cations form a second interpenetrating cubic sub-lattice located at 12-fold coordinated sites between the octahedra. The different principles of chemistry which can be combined (*viz.* ionic radii, valence state, tolerance factor, *etc*.) to obtain numerous complex perovskite oxides with the mixed-cation formula such as (A′A″…)BO$_3$, A(B′B″…)O$_3$ or (A′A″…)(B′B″…)O$_3$ have a variety of interesting properties, designed for many electronic and/or microelectronic devices [Takenaka and Nagata, 2005; Shrout and Zhang, 2007; Panda, 2009; Rödel et al., 2009; Eichel and Kungl, 2010; Damjanovic, 2010]. Also, it has been observed that modifications either at *A*- or *B*-site plays an important role in tailoring various properties of complex perovskites as the material's properties depend mainly on the size difference of pseudo-cation (A′A″…)$^{2+}$ and/or (B′B″…)$^{4+}$ and on the difference on their valance states. It was noticed that rare-earth (RE) based niobates/tantalates having the general formula Ba(RE$_{1/2}$Nb$_{1/2}$)O$_3$/Ba(RE$_{1/2}$Ta$_{1/2}$)O$_3$ are especially useful for microwave applications such as dielectric resonators in wireless communication systems, global positioning systems, cellular phones, *etc.* [Zurmuhlen et al., 1995a; Zurmuhlen et al., 1995b; Ikawa and Takemoto, 2003; Khalam et al., 2004; Dias et al., 2006]. Among these, Ba(Gd$_{1/2}$Nb$_{1/2}$)O$_3$ (abbreviated hereafter as BGN) belongs to perovskite family with cubic symmetry at ambient temperature. Recently, preparation, characterization and microwave dielectric properties of BGN ceramic have been carried out by Khalam et. al. [2004]. In another study, the evaluation of crystal structure and phonon modes of BGN was taken up by Dias et. al. [2006] while Kumar et. al. [2011] studied the electrical properties of BGN having the tetragonal structure. However, the information about the electrical properties of BGN is still not complete and consistent.

The study of electrical conductivity in such materials is very important since the associated physical properties are dependent on the nature and magnitude of conductivity. Residual conductivity in the bulk of the grains of such materials has been found to be ~10^{-7} S m^{-1} in the operating temperature region. The high insulating property is caused mainly due to the fact that grain boundaries in the dielectric material act as highly resistive barriers for the cross transport of charge carriers. Therefore, to have proper understanding about the effect of grain boundaries for evaluating overall behaviour of the ceramic samples is important. Complex impedance spectroscopy technique is considered to be a promising non-destructive testing

method to analyze the electrical processes occurring in a material on the application of small ac signal as input perturbation. The output response of polycrystalline compound plotted in a complex plane, represents grain, grain boundary and electrode/ interface properties with different time constants, leading to successive semicircles. Thus, the dynamics of ionic movement and contributions of various microstructure elements such as grain, grain boundary and interface polarization to total electric response in polycrystalline solids can be identified by this technique. It also enables us to evaluate the nature of dielectric relaxation and the relaxation frequency of the material. Therefore, to have knowledge about the performance of BGN, it becomes important to know the carrier transport mechanism and hence the system deserves further investigation. Accordingly, the present work is an attempt to study the role of grain and grain boundaries on the electrical behaviour of Ba(Gd$_{1/2}$Nb$_{1/2}$)O$_3$ and their dependence on temperature and frequency using complex impedance spectroscopy technique. The structural (X-ray and its Rietveld analysis), microstructural (SEM and EDAX), dielectric, impedance and ac conductivity studies of BGN ceramic have been presented. Also, an attempt has been made to explain the conduction mechanism in the system.

Materials and Methods

Polycrystalline Ba(Gd$_{1/2}$Nb$_{1/2}$)O$_3$ having the tolerance factor ($t = [(r_{Ba} + r_O)/\sqrt{2}][(r_{Gd} + r_{Nb})/2 + r_O]^{-1}$; here r_{Ba}, r_{Gd}, r_{Nb} and r_O are the ionic radii of the constituent ions) 0.97725, was prepared from AR grade (99.9%+ pure, Merck) raw powders of BaCO$_3$, Gd$_2$O$_3$ and Nb$_2$O$_5$ using solid-state reaction process. The raw powders in stoichiometric ratio were mixed in alcohol medium for 2 h, then calcined at 1375°C in air atmosphere for 5 h after drying. The calcined powders added with 5% polyvinyl alcohol, were pressed into the cylindrical pellets of 10 mm in diameter and 1.5–2 mm in height under an uniaxial pressure of 650 MPa. Finally, the dense BGN ceramics were obtained by sintering at 1400°C in air for 4 h. Fig. 1 illustrates entire temperature profile for the preparation of Ba(Gd$_{1/2}$Nb$_{1/2}$)O$_3$ ceramic. Completion of reaction and formation of the desired compound were checked by X-ray diffraction (XRD) technique.

The crystal structure was identified by powder XRD analysis with CuK_α radiation (XPERT-PRO, Pan Analytical). The XRD data for Rietveld analysis were collected over the range of $2\theta = 25° – 90°$ with a step

size of 0.02° and a count time of 2s. The FULLPROF program was used for Rietveld structural refinement. The average crystallite size and the lattice strain of BGN were estimated by analyzing the broadening of XRD peaks, using Williamson–Hall approach: $B\cos\theta = (K\lambda/D) + 2(\Delta\xi/\xi)\sin\theta$; where B is diffraction peak width at half intensity and $\Delta\xi/\xi$ is the lattice strain and K is the Scherrer constant (= 0.89). The term $K\lambda/D$ represents the Scherrer particle size distribution. The microstructure and energy dispersive X-ray (EDAX) pattern was obtained by a scanning electron microscopy (SEM Hitachi S-3400N, Japan) on the fractured surface. For electrical characterization, the samples were polished and a silver electrode paste (SPI, Structure probe, INC.) was applied. The real and imaginary parts of the electrical impedance were measured as a function of frequency (1 Hz ≤ f ≤ 1 MHz) between 50 and 450°C at a heating rate of 1°C/min with a computer interfaced Solartron SI1260 impedance/gain phase analyzer. The real and imaginary parts ac conductivity data were obtained using the relations: $\sigma' = \omega\varepsilon_o\varepsilon''$ and $\sigma'' = \omega\varepsilon_o\varepsilon'$; where ε' and ε'' are the real and imaginary parts of the dielectric constant respectively.
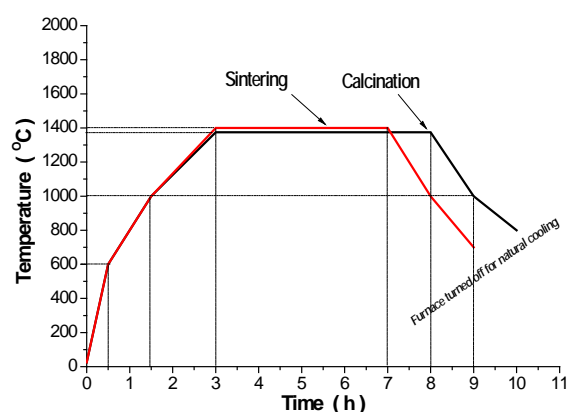

FIG. 1 TEMPERATURE PROFILE FOR THE PREPARATION OF Ba(Gd$_{1/2}$Nb$_{1/2}$)O$_3$ CERAMIC

Results and Discussion

The XRD profile for BGN ceramic is presented in Fig. 2. The results of Rietveld analysis revealed a cubic (fcc) crystal structure having the space group $Pm\bar{3}m$(221) with the unit cell edge length a = 4.2418 Å which was in good agreement with the literature report (ICDD: #89-3100). The experimental parameters of XRD and the refined structural parameters are given in Table 1. The inset of Fig. 2 shows the Williamson-Hall plot for BGN. A linear least square fitting to $B\cos\theta$–$\sin\theta$ data yielded the values of average crystallite size and lattice strain, respectively, to be 170.31 nm and 0.0072.
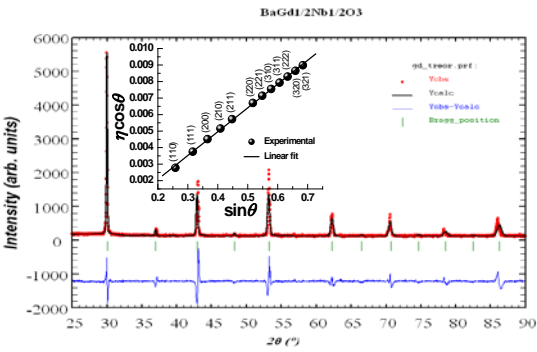
FIG. 2 RIETVELD REFINED PATTERN OF Ba(Gd$_{1/2}$Nb$_{1/2}$)O$_3$ IN SPACE GROUP $Pm\bar{3}m$. SYMBOLS REPRESENT OBSERVED DATA POINTS AND SOLID LINES THEIR RIETVELD FIT INSET: WILLIAMSON–HALL PLOT

TABLE 1 THE CRYSTAL DATA AND REFINEMENT FACTORS OF Ba(Gd$_{1/2}$Nb$_{1/2}$)O$_3$ CERAMIC OBTAINED FROM XRD DATA

Cearmics	BaGd$_{1/2}$Nb$_{1/2}$O$_3$
Crystal System	Cubic
Space group	$Pm\bar{3}m$
a (Å)	4.2418
V (Å^3)	76.4337
R_P	33.5
R_{wp}	31.2
R_{exp}	17.3
R_B	0.0154
R_F	0.0397
χ^2	3.248
d	0.7321
Q_D	1.8891
S	1.80

Fig. 3 shows the SEM image and EDAX pattern of fractured surface of sintered BGN. All the peaks in the EDAX pattern have been perfectly assigned to the elements present in Ba(Gd$_{1/2}$Nb$_{1/2}$)O$_3$, which indicates the purity of chemical composition of BGN. The scanning electron micrograph of the sample is shown in the inset of Fig. 3. The nature of the micrographs exhibits the polycrystalline texture of the material and grains are distributed throughout the sample. The average grain size of the sintered sample were estimated to be ~ 1 μm.
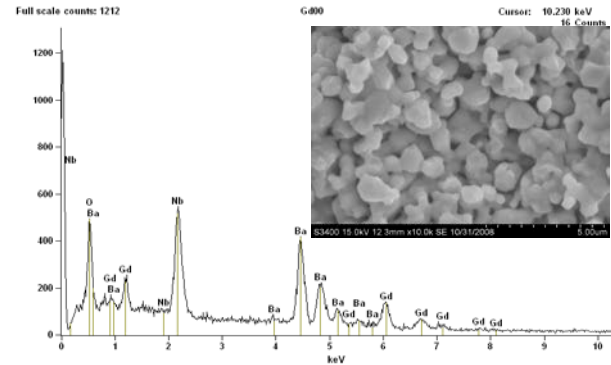

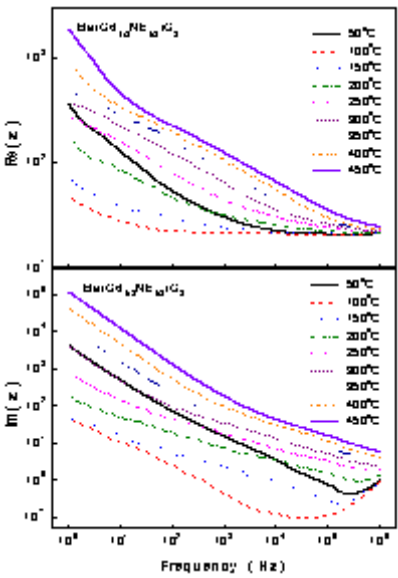FIG. 3 EDAX SPECTRUM AND SEM IMAGE (INSET) OF Ba(Gd$_{1/2}$Nb$_{1/2}$)O$_3$ CERAMIC

FIG. 4 FREQUENCY DEPENDENCE OF REAL AND IMAGINARY PARTS OF PERMITTIVITY OF Ba(Gd$_{1/2}$Nb$_{1/2}$)O$_3$ CERAMIC AT DIFFERENT TEMPERATURES
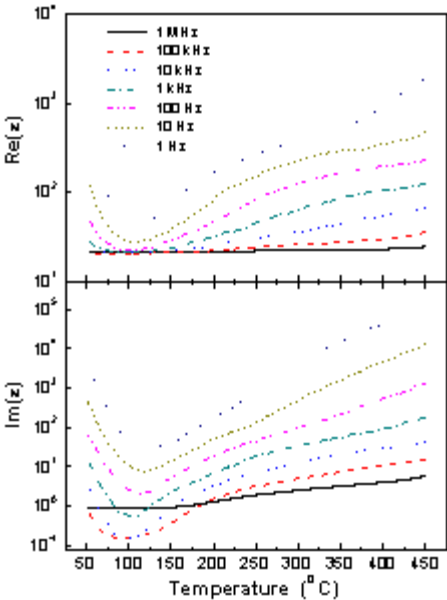

FIG. 5 TEMPERATURE DEPENDENCE OF REAL AND IMAGINARY PARTS OF PERMITTIVITY OF Ba(Gd$_{1/2}$Nb$_{1/2}$)O$_3$ AT DIFFERENT FREQUENCIES

The frequency dependence of real (ε') and imaginary (ε'') parts of permittivity for BGN ceramics at different temperatures is shown in Fig. 4. It is observed that the values of both ε' and ε'' decrease with increasing frequency. It is known that the variations in ε' and ε'' are attributed to different types of polarizations $e.g.$, ionic, electronic, dipolar and space charge or interfacial which arise at different stages of material's response to varying temperature and frequency of the applied alternating field, each of which involves a short range displacement of charges and contributes to the total polarization and hence to the permittivity of the material. The observed

dielectric response is similar to the other compounds of the family [Amar Nath et al., 2013; Prasad et al., 2010a; Prasad et al., 2010b].

The temperature variation of ε' and ε'' for BGN ceramic at different frequencies are given in Fig. 5. The values of both ε' and ε'' were found to first decrease and then they increase with the rise in temperature. Also, the room temperature values of ε' and ε'' is found to be 30 and 15, respectively, at 1 kHz. This result is in consistent with the general observation that the dielectric constants for materials having cubic structures are, in general, very small [Amar Nath et al., 2013; Prasad et al., 2010a]. Also, no phase transition was observed in the chosen temperature range.
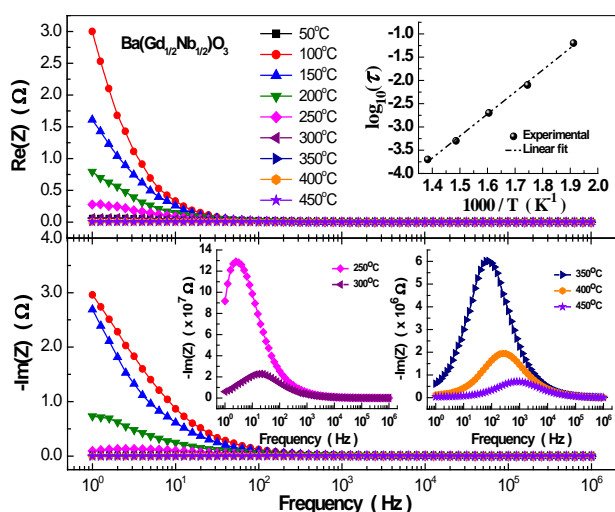

FIG. 6 FREQUENCY DEPENDENCE OF REAL AND IMAGINARY PARTS OF IMPEDANCE OF Ba(Gd$_{1/2}$Nb$_{1/2}$)O$_3$ CERAMIC AT DIFFERENT TEMPERATURES. INSETS: TEMPERATURE DEPENDENCE OF RELAXATION TIME AND EXPANDED VIEW OF IMAGINARY PART OF IMPEDANCE

The logarithmic frequency dependence of Z' and Z'' of BGN, at different temperatures are plotted in Fig. 6. It is observed that the values of Z' decreases monotonically with increasing frequency up to certain frequency and then becomes almost frequency independent for all temperatures. Also, the value of Z' decreases with the rise of temperature indicating thereby the negative temperature coefficient of resistance (NTCR) character of BGN. Further, at lower temperatures, Z'' decreases monotonically suggesting the absence of any relaxation. This suggests that the relaxation species are immobile defects and the orientation effect might be associated. As the temperature increases (from 250°C onwards), the peak of Z'' starts appearing (insets of Fig. 6), which shifts towards higher frequency side with the increment in temperature, showing that the resistance of the bulk material is decreasing and supports NTCR character of

BGN. Besides, the magnitude of Z'' peaks decreases while the width of the peak increases with increasing temperature. Also, the peaks are slightly asymmetric in nature, which suggests that there is a spread of relaxation times *i.e.* the existence of a temperature dependent electrical relaxation in the material [Prasad et al., 2009]. Furthermore, the relaxation time (τ) was calculated from the frequency at which peak was observed. At the peak ($\omega = \omega_0$), the most probable relaxation is defined by the condition: $\omega \tau = 1$. It is found that the relaxation time obeys the Arrhenius relationship: $\tau = \tau_0 \exp(-U / k_B T)$, where τ_0 is the pre-exponential factor and U is the activation energy. The inset of Fig. 6 shows a plot of log τ *vs.* $1/T$. The value of U is estimated to be 0.408 eV using linear least squares fit to the data points shown in inset of Fig.6.
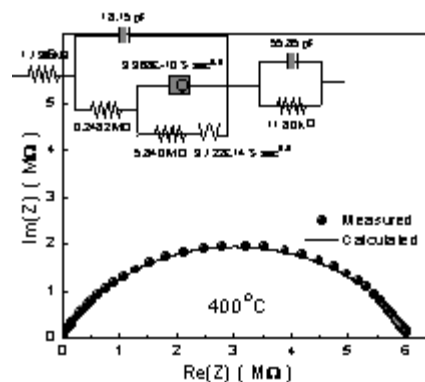

FIG. 7 COMPLEX IMPEDANCE PLOT OF Ba(Gd$_{1/2}$Nb$_{1/2}$)O$_3$ CERAMIC AT 400°C. INSET: APPROPRIATE EQUIVALENT ELECTRICAL CIRCUIT

Fig. 7 illustrates a complex impedance plot along with the appropriate equivalent circuit (inset) and it's fitting at 400°C. Equivalent circuit (inset Fig. 7) of type R$_1$(C$_2$(R$_2$(Q(R$_3$W))))(C$_4$R$_4$); where R, C, Q and W, are resistance, capacitance, constant phase element and Warburg element, respectively, fitting excellently well with the impedance data, which clearly indicates the grain and grain boundary contributions. The fitting parameters were determined using a non-linear least-square fitting algorithm and indicated in the equivalent circuit. A constant phase element appeared in the equivalent circuit may be due to the surface roughness and the Warburg impedance element could be due to the semi-infinite linear diffusion *i.e.* unrestricted diffusion to a large planar electrode, which obeys second Fick's law [Prasad et al., 2010b]. Also, it can be seen that the centre of semicircles lie little below the Z' -axis, which clearly suggests the non-Debye nature of dielectric relaxation in BGN, similar to Ba(Pr$_{1/2}$Nb$_{1/2}$)O$_3$ [Amar Nath et al., 2013], Ba(Y$_{1/2}$Nb$_{1/2}$)O$_3$ [Prasad et al., 2010a] and Ba(La$_{1/2}$Nb$_{1/2}$)O$_3$ [Prasad et al., 2010b].
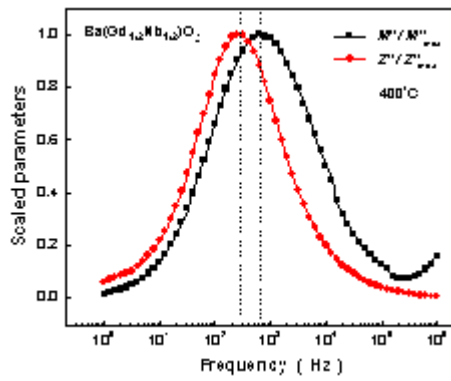
FIG. 8 VARIATION OF SCALED PARAMETERS OF
Ba(Gd$_{1/2}$Nb$_{1/2}$)O$_3$ CERAMIC

The variation of scaled parameters (Z''/Z''_{max} and M''/M''_{max}) with frequency at 400°C is illustrated in Fig. 8. It is observed that the peaks do not occur at the same frequency and following the sequence $f_{Z''} < f_{M''}$, which provides an evidence of presence of apparent polarization. This indicates the short-range conductivity of charge carrier *via* hopping type of mechanism [Gerhardt, 1994].
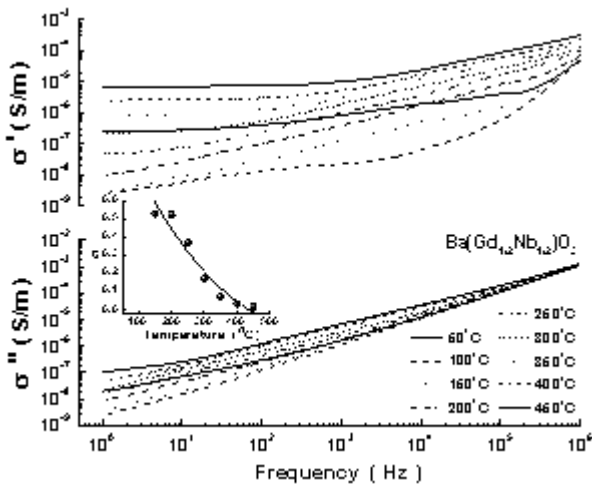

FIG. 9 VARIATION OF REAL AND IMAGINARY PARTS OF AC
CONDUCTIVITY WITH FREQUENCY AT DIFFERENT
TEMPERATURES FOR Ba(Gd$_{1/2}$Nb$_{1/2}$)O$_3$ CERAMIC. INSET:
VARIATION OF INDEX 's' WITH TEMPERATURE

Fig. 9 shows the variation of real (σ') and imaginary (σ'') parts of ac conductivity of BGN as a function of frequency at different temperatures between 50°C and 450°C. The imaginary part of the ac conductivity decreases with decreasing frequency and at higher temperature it finds almost plateau value in lower frequency side. It is known that ac conductivity of the system depends on the dielectric properties. The nature of variation of σ' with frequency exhibits conductivity dispersion throughout the chosen frequency range. Also, the values of σ' increase with rise in frequency as well as temperature. Such increment in conductivity is due to the movement of

thermal ions (generally comes from hopping motion of ions) from one preferable site to the other. As the temperature rises, the plots get flattened (low frequency plateau). The high-frequency conductivity dispersion may be attributed to ac conductivity whereas the frequency independent plateau region of the conductivity pattern corresponds to the dc conductivity (σ_{dc}) of the material. The switch from frequency-independent to the frequency-dependent region shows the onset of the conductivity relaxation phenomenon which shifts to higher frequency side with the increase of temperature, indicating the translation from long range hopping to the short range ion motion. Furthermore, the real part of electrical conductivity, in most of the materials due to localized states is expressed as a Jonscher's power law [Grigas, 1996]: $\sigma' = \sigma_o + A\omega^S$. The values of the index *s* have been obtained from the slopes of the plots in the low frequency region, which always comes out to be less than 1 and decrease with the rise in temperature (inset Fig. 9), which is consistent with correlated barrier hopping model. Therefore, the electrical conduction in the system may be considered due to the short range translational type hopping of charge carriers. Besides, the value of *s* approaching to zero at higher temperatures indicates that the dc conductivity dominates at higher temperatures in the low frequency region following the Jonscher's power law.
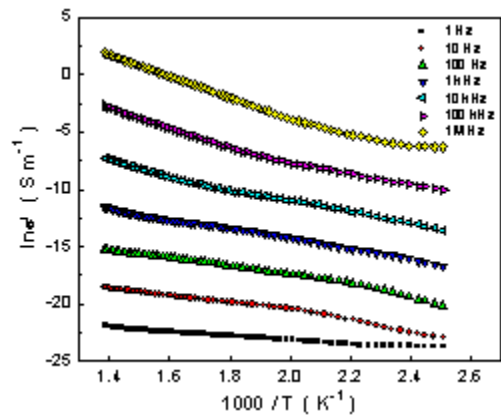

FIG. 10 VARIATION OF REAL PART OF AC CONDUCTIVITY
WITH TEMPERATURE AT DIFFERENT FREQUENCIES FOR
Ba(Gd$_{1/2}$Nb$_{1/2}$)O$_3$ CERAMIC

Fig. 10 shows the variation of ac conductivity versus $10^3/T$. The plots show the NTCR behaviour of BGN. The apparent activation energy for conduction was obtained from high temperature region using the Arrhenius relationship $\sigma' = \sigma_o \exp(-E_a/k_B T)$. A linear least square fitting of the ac conductivity data was given the values of the apparent activation energy E_a to be 0.25, 0.17 and 0.074 eV at 1 Hz, 1 kHz and 1 MHz, respectively. The low value of E_a may be due to the

carrier transport through hopping between localised states in a disordered manner.

Conclusions

Polycrystalline Ba(Gd$_{1/2}$Nb$_{1/2}$)O$_3$ prepared using high temperature solid state reaction method, was found to possess a perovskite type cubic structure with the space group $Pm\overline{3}m(221)$. The dielectric relaxation was found to be of non-Debye type; while the ac conductivity was found to obey the universal power law and showed the NTCR character.

REFERENCES

Takenaka, T., and Nagata, H. "Current status and prospects of lead-free piezoelectric ceramics." Journal of the European Ceramic Society 25 (2005): 2693-700.

Shrout, T.R., and Zhang, S.J. "Lead-free piezoelectric ceramics: Alternatives for PZT?." Journal of Electroceramics 19 (2007): 111-24.

Panda, P.K. "Review: environmental friendly lead-free piezoelectric materials." Journal of Materials Science 44 (2009): 5049-62.

Rödel, J. et al. "Perspective on the development of lead-free piezoceramics.". Journal of the American Ceramic Society 92 (2009): 1153-77.

Eichel, R.–A., and Kungl, H. "Recent developments and future perspectives of lead-free ferroelectrics." Functional Matrrials Letters 3 (2010): 1-4.

Damjanovic, D. et al. "What can be expected from lead-free piezoelectric materials?.". Functional Matrrials Letters 3 (2010): 5-13.

Zurmuhlen, R. et al. "Dielectric spectroscopy of Ba(B$'_{1/2}$B$''_{1/2}$)O$_3$ complex perowskite ceramics: Correlations between ionic parameters and microwave dielectric properties. I. Infrared reflectivity study (10^{12}-10^{14} Hz)." Journal of Applied. Physics 77 (1995a): 5341-50.

Zurmuhlen, R. et al. "Dielectric spectroscopy of Ba(B$'_{1/2}$B$''_{1/2}$)O$_3$ complex perovskite ceramics: Correlations between ionic parameters and microwave dielectric properties. II. Studies below the phonon eigenfrequencies (10^2-10^{12} Hz)." Journal of Applied. Physics 77 (1995b): 5351-64.

Ikawa, H., and Takemoto, M. "Products and microwave dielectric properties of ceramics with nominal compositions (Ba$_{1-x}$Ca$_x$)(B$_{1/2}$B$'_{1/2}$)O$_3$ (B = Y^{3+}, Nd^{3+}, Gd^{3+}; B' = Nb^{5+}, Ta^{5+})." Materials Chemistry and Physics 79 (2003): 222-25.

Khalam, L.A. et al. "Preparation, characterization and microwave dielectric properties of Ba(B$'_{1/2}$Nb$_{1/2}$)O$_3$ [B' = La, Pr, Nd, Sm, Eu, Gd, Tb, Dy, Ho, Y, Yb and In] ceramics." Materials Science and Engineering: B 107 (2004): 264-70.

Dias, A. et al. "Chemical Substitution in Ba(RE$_{1/2}$Nb$_{1/2}$)O$_3$ (RE) La, Nd, Sm, Gd, Tb, and Y) Microwave Ceramics and Its Influence on the Crystal Structure and Phonon Modes." Chemistry of Materials 18 (2006): 214-220.

Kumar, P. et al. "X-ray and electrical properties of Ba(Gd$_{0.5}$Nb$_{0.5}$)O$_3$ ceramic." Advanced Materials Letters 2 (2011): 76-81.

Amar Nath, K. et al. "Impedance and ac conductivity studies of Ba(Pr$_{1/2}$Nb$_{1/2}$)O$_3$ ceramic." Bulletin of Material Science 36 (2013): 591-99.

Prasad, K. et al. "Electrical properties of BaY$_{0.5}$Nb$_{0.5}$O$_3$ ceramic: Impedance spectroscopy analysis." Physica B: Condensed Matter 405 (2010a): 3564-71.

Prasad, K. et al. "Structural and electrical properties of lead-free ceramic: Ba(La$_{1/2}$Nb$_{1/2}$)O$_3$." Advances in Applied Ceramics 109 (2010b): 225-33.

Prasad, K. et al. "Dielectric relaxation in lead-free perovskite Ba(Bi$_{1/2}$Nb$_{1/2}$)O$_3$." Physica Status Solidi (a) 206 (2009): 316-20.

Gerhardt, R. "Impedance and dielectric spectroscopy revisited: Distinguishing localized relaxation from long-range conductivity." Journal of Physics and Chemistry of Solids 55 (1994): 1491-506.

Grigas, J., Microwave Dielectric Spectroscopy of Ferroelectrics and Related Materials. Amsterdam: Gordon and Breach Publn. Inc., 1996.

Kumar Amar Nath has obtained his Ph.D. degree in 2011. He has more than 10 years of research experience and working as Scientist. One patent has been published in the Indian Patent Journal for the improvement in quality of graphite nipple with his name to Indian Patent Office. He is author/co-author of more

than 10 research papers in different national and international journals. He has also authored a book titled Knowledge Management in Corporate Sector, which is published by LAP LAMBERT Academic Publishing GmbH & Co. KG, Germany.

K. P. Chandra graduated from T.M. Bhagalpur University, Bhagalpur, India in 1994 with an M.Sc in Physics, and Ph.D. degree from D.D.U. Gorakhpur University, Gorakhpur, India. Presently, he is working as Assistant Professor at the S.M. College, Bhagalpur under T.M. Bhagalpur University in Bhagalpur, India. His research interest includes the study of organic materials, ferroelectrics and biogenic materials. He has published over thirty research papers in reputed international journals.

A. R. Kulkarni, M.Sc., Ph.D. is Professor at the Department of Metallurgical Engineering & Materials Science, I. I. T. Bombay, Mumbai, India. He has more than 150 publications, three books, one patent and a technology transfer to his credit and has supervised more than 10 Ph.D. and 35 M.Tech. students. He is actively associated with different scientific societies and journals as a peer and editorial board member. He has handled several national/international research projects, and has honoured with many prestigious national/international awards. His current areas of research are Electroceramics, Thin Films, Glass-ceramics, Solid Electrolytes, Ion-Dynamics in Glasses, IR-Transmitting Glasses.

K. Prasad, M.Sc., PGDCA, Ph.D. is Professor and Head at the Aryabhatta Centre for Nanoscience and Nanotechnology, Aryabhatta Knowledge University, Patna, India. He also served SLIET, Longowal (Punjab), T.M. Bhagalpur University, Bhagalpur, and Central University of Jharkhand, Ranchi, India. His current research interests include ferroelectric/piezoelectric ceramics and ceramic-polymer composites and synthesis of advanced nanomaterials through soft-chemical and biosynthetic routes. He has (co-) authored over 150 publications including a book and three book chapters. He is also member of editorial board and peer of different international journals. Dr. Prasad has successfully guided six Ph.D. students. He has presented papers and delivered invited lectures at major national/international conferences.